THE JOURNAL OF BIOLOGICAL CHEMISTRY
Vol. 275, No. 36, Issue of September 8, pp. 27775–27783, 2000

Printed in U.S.A.

Phosphorylation Site Analysis of Semliki Forest Virus Nonstructural Protein 3*

Received for publication, March 16, 2000, and in revised form, June 7, 2000
Published, JBC Papers in Press, June 12, 2000, DOI 10.1074/jbc.M002195200

Helena Vihinen‡§ and Juhani Saarinen¶

From the ‡Program in Cellular Biotechnology and ¶Protein Chemistry Laboratory, Institute of Biotechnology, Viikki Biocenter, University of Helsinki, Helsinki FIN-00014, Finland

Nonstructural protein 3 (Nsp3) is an essential subunit of the alphavirus RNA replication complex, although its specific function(s) has yet to be well defined. Previously, it has been shown that Semliki Forest virus Nsp3 (482 amino acids) is a phosphoprotein, and, in the present study, we have mapped its major phosphorylation sites. Mass spectrometric methods utilized included precursor ion scanning, matrix-assisted laser desorption/ionization mass spectrometry used in conjunction with on-target alkaline phosphatase digestions, and tandem mass spectrometry. Two-dimensional peptide mapping was applied to separate tryptic ^{32}P-labeled phosphopeptides of Nsp3. Radiolabeled peptides were then subjected to Edman sequencing, and phosphoamino acid analysis. In addition, radiolabeled Nsp3 was cleaved successively with cyanogen bromide and trypsin, and microscale iron-chelate affinity chromatography was used to enrich phosphopeptides. By combining these methods, we showed that Nsp3 is phosphorylated on serine residues 320, 327, 332, 335, 356, 359, 362, and 367, and is heavily phosphorylated on peptide Gly^{338}–Lys^{415}, which carries 7–12 phosphates distributed over its 13 potential phosphorylation sites. These analytical findings were corroborated by constructing a Nsp3 derivative devoid of phosphorylation. The results represent the first determination of phosphorylation sites of an alphavirus nonstructural protein, but the approach can be utilized in phosphoprotein analysis in general.

The phosphorylation and dephosphorylation of proteins play a crucial role in the regulation of many cellular processes. In viral systems, the phosphorylation of specific proteins modulates virus replication and virus-host interactions (1). For example, the phosphorylation of the P protein in several negative-strand RNA viruses has been found to be essential for the viral transcription activity (2, 3).

Alphaviruses, such as Semliki Forest virus (SFV),[1] Sindbis virus (SIN), and Venezuelan equine encephalitis virus, are enveloped positive-strand RNA viruses capable of causing disease in mammals including man. The RNA genome of SFV (total length ~11.5 kilobases) codes for two polyproteins, nonstructural and structural. The nonstructural polyprotein (P1234), is autoproteolytically cleaved into the four nonstructural proteins Nsp1–Nsp4 (reviewed in Refs. 4 and 5). Recently, studies have shown that SFV Nsp1 has nucleotide methylation and viral mRNA capping functions (6, 7). Nsp2 was found to be the autoprotease responsible for the cleavage of the nonstructural polyprotein (8), an RNA helicase (9), and an RNA triphosphatase (10). As for Nsp4, protein sequence homology with other viral proteins of known function suggests that Nsp4 is the catalytic subunit of the SFV RNA-dependent RNA polymerase (11). Whereas functions have been determined for the other nonstructural proteins, the function of Nsp3 remains poorly characterized. Studies of SIN polyprotein processing intermediates containing Nsp3 have shown that it is essential for the synthesis of negative-strands during the early phase of RNA replication (12, 13). In addition, SIN Nsp3 has been reported to putatively affect the synthesis of subgenomic mRNA encoding the virus structural proteins (14, 15).

Amino acid sequence comparisons suggest that N-terminal regions of alphavirus Nsp3s are highly conserved sharing significant similarity with rubella virus, hepatitis virus E, and coronavirus sequences (16). Furthermore, a recent genomic analysis has revealed that sequences related to the Nsp3 N-terminal domain are widely found in bacteria, animals, and plants (17). The conservation of this region during evolution suggests an important and basic function for this domain, which for the moment remains unclear. In contrast, the C-terminal region of Nsp3 is not conserved among alphaviruses and varies both in sequence and in length from 134 aa in Middelburg virus to 246 aa in O'nyong-nyong virus (5). However, some similarities do exist in the C-terminal domains of alphaviruses, *e.g.* all are rich in acidic residues, as well as in serine and threonine, and devoid of any predicted secondary structure. It appears that Nsp3 is the only alphavirus nonstructural protein, which is modified by phosphorylation (18, 19). Phosphoamino acid analysis of SFV Nsp3 (total of 482 aa) showed that serine and threonine residues are phosphorylated in the approximate ratio of 2:1 (18), but the exact positions of phosphorylated Nsp3 residues have not been reported. The identification of phosphorylation sites in Nsp3 is important for a number of reasons including: determining whether Nsp3 phosphorylation sites are constant or changed during virus evolution, mapping potential changes in phosphorylation pat-

* This work was supported by Academy of Finland Grant 8397, the Technology Development Center, and the Helsinki University Foundation. The costs of publication of this article were defrayed in part by the payment of page charges. This article must therefore be hereby marked "*advertisement*" in accordance with 18 U.S.C. Section 1734 solely to indicate this fact.

§ To whom correspondence should be addressed: Inst. of Biotechnology, P.O. Box 56, Viikinkaari 9, University of Helsinki, Helsinki FIN-00014, Finland. Tel.: 358-9-19159650; Fax: 358-9-19159560; E-mail: helena.vihinen@helsinki.fi.

[1] The abbreviations used are: SFV, Semliki Forest virus; SIN, Sindbis virus; Nsp, nonstructural protein; CID, collision-induced dissociation; PVDF, polyvinylidene difluoride; ESI, electrospray ionization; MS, mass spectrometry; ACN, acetonitrile; CNBr, cyanogen bromide; THAP, 2,4,6-trihydroxyaceptophenone; CIP, calf intestinal alkaline phosphatase; MALDI, matrix-assisted laser desorption/ionization; TOF, time-of-flight; TLC, thin layer chromotography; TLE, thin layer electrophoresis; wt, wild type; aa, amino acid(s); PAGE, polyacrylamide gel electrophoresis; PCR, polymerase chain reaction; RP, reverse phase; HPLC, high performance liquid chromatography; BHK, baby hamster kidney.

terns during alphavirus infection in different tissues, and determining potential phosphorylation sites for future mutagenesis studies. Furthermore, because information regarding phosphorylation sites in SFV Nsp3 represents the first systematic mapping of such sites in alphaviruses, it would represent a model for other related pathogenic viruses.

Detailed characterization of protein phosphorylation is hampered by the low amount of material available for analysis, and by the fact that the stoichiometry of protein phosphorylation is often very low, *i.e.* the phosphopeptides exist as a minor fraction in a large background of unphosphorylated peptides. Advances in ionization methodologies (electrospray and matrix-assisted laser desorption/ionization (MALDI)) have made biological mass spectrometry effective and sensitive enough for studying posttranslational protein modifications (20, 21). Recently, mass spectrometric methods for phosphorylation analysis after SDS-PAGE separation have been described (22, 23). Although mass spectrometry has become a very efficient tool in the identification of phosphopeptides, problems still remain. For example, when a peptide contains multiple phosphates and many potential phosphorylation sites, the site-specific identification of phosphorylated residues is often limited by the fact that multiply phosphorylated peptides are likely to produce very complex collision-induced decomposition (CID) spectra, or ionize poorly in the positive ion mode. SFV Nsp3 is a challenging molecule for phosphorylation studies, since it has relatively high number of potential phosphorylation sites (39 Ser and 35 Thr residues), and the protein is somewhat resistant to enzymatic cleavage. However, by using the mass spectrometric methods along with two-dimensional phosphopeptide mapping and Edman sequencing, we were able to map the major, if not all, phosphorylation sites of Nsp3. Based on these results, we constructed a deletion/point mutation derivative of Nsp3, which could not be phosphorylated as judged by loss of ^{32}P incorporation, thus further supporting the validity of phosphorylation site analysis.

EXPERIMENTAL PROCEDURES

Plasmid Construction—Deletion and point mutations were made in the *NSP3* coding region, which was originally cloned into plasmid pTSF3 under the control of the T7 promoter (24). A deletion mutant, which had amino acids between 342 and 369 of Nsp3 removed, was made using PCR with the following primers: 1, 5′-CTCAAGCTTATGCACCCGCGCGGCCTAGTCG-3′; 2, 5′-ATCACCATGGCACCATCCTACAGAGTTAAG-3′; 3, 5′-TCGTAGTCCAAGTCAAACCCTCGTAACGACCGATC-3′; 4, 5′-TGGACTACGAGCCAATGGCTCCCATAGTAGTGACGG-3′. The PCR products were purified and used as templates in a second round of PCR with primers 2 and 4. Serine residues 320, 327, 332, and 335 were mutated to alanine by using a site-directed mutagenesis kit (U.S.E. kit, Amersham Pharmacia Biotech) according to the manufacturer's instructions. A Nsp3 mutant containing both the 343–368 deletion and the four point mutations was designated Nsp3Δ26+4S→4A. All sequence alterations were verified by DNA sequencing.

Expression and Metabolic Labeling in HeLa Cells—HeLa cell monolayers were grown in Dulbecco's modified minimal essential medium supplemented with 10% heat-inactivated fetal calf serum, and 100 units/ml streptomycin and penicillin. The modified vaccinia virus Ankara was kindly provided by Dr. B. Moss (National Institutes of Health, Bethesda, MD), and virus stocks were made as described previously (25). HeLa cell dishes that were 80–90% confluent were infected with virus using 20–50 plaque-forming units/cell. After a 45-min adsorption period, the cells were washed, and transfected using Opti-MEM (Life Technologies, Inc.), the pTSF3 plasmid or its derivatives, and Lipofectin (Life Technologies, Inc.). Transfection mixtures of 7 μg of DNA in 12 μl of Lipofectin, and 10 μg of DNA in 50 μl of Lipofectin were used for 60- and 100-mm plates, respectively. After 3–4 h, the transfection mixture was replaced with medium containing 0.2% bovine serum albumin. Cells were then incubated for 1–3 h at 37 °C. For *in vivo* labeling, transfected cells were washed twice at 2 h after transfection with Dulbecco's medium containing 0.2% bovine serum albumin, after which methione/cysteine-free or phosphate-free medium was added. Cells were labeled at 3 h after transfection either with 150 μCi of [^{35}S]methionine/cysteine (>1000 Ci/mmol, Redivue PRO-mix, Amersham Pharmacia Biotech) or with 300–1000 μCi of carrier-free [^{32}P]orthophosphate (10 mCi/ml, Amersham Pharmacia Biotech) per plate. After 3–5 h at 37 °C, cells were washed carefully, harvested, and lysed in 1% SDS.

Immunoprecipitation, SDS-PAGE, and Immunoblotting—HeLa cells were lysed in phosphate-buffered saline containing 1% SDS, 10 mM sodium fluoride (Merck), and a protease inhibitor mixture at a recommended concentration (Complete™; Roche Molecular Biochemicals). After shearing the DNA by drawing the lysate repeatedly through a 27-gauge needle, the proteins were denatured by boiling, and Nsp3 was immunoprecipitated with anti-Nsp3 rabbit antiserum, as described previously (18). Proteins were separated in 10% SDS-PAGE gels, and electrotransferred to nitrocellulose (Hybond-C Extra, Amersham Pharmacia Biotech) or polyvinylidene difluoride membrane (PVDF; Immobilon, Millipore) as described previously (6). For phosphopeptide mapping analysis, samples were alkylated in 10 mM dithiothreitol, 3 mM EDTA, and 20 mM iodoacetamide for 15 min prior to separation by SDS-PAGE. Radiolabeled proteins were detected by using an imaging system (Fuji BAS 1500).

In-gel Digestion of Nsp3 for ESI-MS Analysis—Immunoprecipitated Nsp3 was resolved by 10% SDS-PAGE and detected by Coomassie Blue staining. The Nsp3 band, corresponding to approximately 1 μg of protein (20 pmol), was excised and destained by rinsing the gel pieces twice in 0.1 M NH_4HCO_3 in 50% acetonitrile (ACN) for 45 min at 37 °C. Gel pieces were then dehydrated with 100% ACN and vacuum-dried. Gel pieces were rehydrated in 10 μl of 0.1 M NH_4HCO_3, 10% ACN containing 40 ng/μl trypsin (modified trypsin, sequencing grade, Promega). The trypsin digestion was performed overnight. The samples were desalted by miniature reversed-phase chromatography column as described previously (22) using POROS R2 (Perseptive Biosystems) as absorbent. The sample was eluted with 2 μl of 0.5% ammonia in 50% methanol directly to the nanoelectrospray needle.

Cyanogen Bromide Degradation in SDS-PAGEs—Approximately 5 μg (100 pmol) of ^{32}P-labeled Nsp3 was obtained from a dried gel piece, as described above. Cleavage with cyanogen bromide (CNBr) was performed with 5 mg/ml CNBr in 70% trifluoroacetic acid in the dark for 18 h at room temperature. The peptides were extracted once with 150 μl of aqueous 50% ACN for 30 min at 37 °C, and twice with 150 μl of 5% formic acid in 50% ACN for 45 min at 37 °C. The supernatants were combined and lyophilized. To reduce the amount of CNBr in samples before reversed-phase HPLC, samples were dissolved in 100 μl of deionized water, and lyophilized. This treatment was repeated three times. The peptides were dissolved in 1% trifluoroacetic acid and applied to 37 °C reversed-phase HPLC.

Separation of CNBr Fragments by Reversed-phase HPLC—Peptides resulting from CNBr digestion were separated by reversed-phase HPLC on a 1 × 20-mm C-1 column (TMS-C1, 300 Å, 5 μm; Tosoh Corp.) by elution with a linear gradient of acetonitrile (5–100% in 60 min) in 0.1% trifluoroacetic acid. Chromatography was performed at a flow rate of 50 μl/min, and the elution was monitored by UV absorbance at 214 nm. Fractions were taken at 1-min intervals, and 0.3-μl aliquots were spotted on a PVDF membrane, air-dried, and analyzed for ^{32}P radioactivity by phosphoimaging.

Trypsin Digestion of CNBr Fragments—After reversed phase chromatography of CNBr-digested Nsp3, fractions containing radioactivity were combined into three pools corresponding to their elution time from the C-1 column. Pool 1 contained early eluting radioactive fractions, pool 2 middle eluting fractions, and pool 3 consisted of late eluting components. Each pool was lyophilized and dissolved in 50 μl of digestion buffer (0.1 M NH_4HCO_3 in 10% ACN) containing 0.05 μg/μl trypsin. The digestion was performed at 37 °C for 18 h, after which fractions were lyophilized and dissolved into 10 μl of 1% trifluoroacetic acid. Half of each trypsin-digested pool was subjected to separation by reversed-phase HPLC on a 0.3 × 20-mm C-8 column (Vydac C8, 300 Å, 9 μm). Peptides were eluted with a linear gradient of ACN (5–100% in 60 min) in 0.1% trifluoroacetic acid at a flow rate of 5 μl/min, and elution was monitored by UV absorbance at 206 nm. Fractions were collected every 2 min, and radioactive fractions were identified by phosphoimaging.

Immobilized Metal Chelate Affinity Chromatography—To enrich for phosphorylated peptides, tryptic peptides made from CNBr-digested Nsp3 were applied to a miniature Fe^{3+} column consisting of 0.5 μl of POROS MC (Perseptive Biosystems) packed into a gel-loader pipette tip. The column was equilibrated with 30 μl of equilibration buffer (2:1 v/v mixture of 0.1 M ammonium acetate, pH 3.1, and acetonitrile). One microliter of tryptic/CNBr-digested peptides from all three pools were combined, which represented 10% of the total sample and 10 pmol of Nsp3 protein starting material, diluted 1:10 in equilibration buffer, and

passed through the column. The column was washed with 20 μl of equilibration buffer, and washed again with 20 μl of equilibration buffer diluted 1:10 in H_2O. Peptides were eluted with 5 μl of 0.5% ammonia in 50% methanol and directly applied to the MALDI target plate, as 1-μl fractions.

On-target Alkaline Phosphatase Treatment—After MALDI-time-of-flight (TOF) mass analysis of fractions from Fe^{3+}-chromatography, in both positive and negative ion mode, the samples (prepared on the MALDI target plate with 2,4,6-trihydroxyacetophenone (THAP) matrix, as described below) were dissolved in 0.5 μl of 50 mM NH_4HCO_3, pH 8.9, containing 0.01 units of calf intestinal alkaline phosphatase (CIP, New England Biolabs). Samples were then incubated for 2 h at 37 °C in a high humidity chamber to prevent drying. Dephosphorylation was stopped by the addition of 0.5 μl of ACN, and samples were immediately dried *in vacuo* to allow for proper crystallization of the matrix.

Mass Spectrometry—MALDI-TOF mass spectrometry was performed on a Biflex™ time-of-flight instrument (Bruker-Franzen Analytik, Bremen, Germany) equipped with a nitrogen laser operating at 337 nm. The Fe^{3+}-affinity chromatography fractions, as well as products from the phosphatase reactions were analyzed both in the linear negative ion delayed extraction mode, and reflector positive ion delayed extraction mode, using THAP, 3 mg/ml in acetonitrile with 20 mM aqueous diammonium citrate, 1:1, by volume, as the matrix. Samples were prepared as described previously (26), and all mass spectra were externally calibrated with angiotensin II and adrenocorticotropic hormone corticotropin-like intermediate peptide.

The Nsp3 phosphopeptides isolated by reversed phase chromatography were analyzed in the reflector positive ion delayed extraction mode using an α-cyano-4-hydroxycinnamic acid saturated solution in 0.1% trifluoroacetic acid and 30% acetonitrile as the matrix. Samples were prepared by mixing 0.5 μl of eluate with 0.5 μl of α-cyano-4-hydroxycinnamic acid matrix on the target plate, and dried under a gentle stream of warm air. Mass spectra were calibrated as above.

Electrospray ionization (ESI) precursor ion scan mass spectra were obtained using an API 365 triple quadrupole mass spectrometer (PE-Sciex, Ontario, Canada) with a nanoelectrospray source installed. Q1 scans were acquired with 0.1-Da step width and a dwell time of 1 ms, at 1-unit resolution. Precursor ion scans were acquired with a step width of 0.5 Da, and a dwell time of 50 ms. The resolution was set to transmit a mass window of 4 Da, the collision gas used was nitrogen, and the collision energy was set to 150 V.

Electrospray ionization product ion mass spectra were collected using a Micromass Q-TOF quadrupole/time-of-flight hybrid mass spectrometer (Micromass, Manchester, United Kingdom) with a nanoelectrospray source installed. Product ion scans were acquired with a Q1 resolution set to transmit a mass window of 5 Da. The doubly charged parent ions $[M + 2H]^{2+}$ were selectively transmitted by the first mass analyzer and directed into the collision cell containing argon as the collision gas. Collision energies were adjusted for each experiment individually.

Tryptic Phosphopeptide Mapping—^{32}P-Labeled Nsp3 or its derivatives were immunoprecipitated, resolved by SDS-PAGE, and blotted either onto nitrocellulose or PVDF membrane. PVDF membrane was dried prior to detection by phosphoimaging, but the nitrocellulose membrane was kept moist during the localization of the bands by placing it into a plastic bag. The membrane pieces were excised and saturated with 0.5% polyvinylpyrrolidone 360 at 37 °C for 1 h. The membrane pieces were washed several times with 10% ACN, and the protein was digested with trypsin in 50 mM NH_4HCO_3 in 10% ACN. After overnight incubation at 37 °C, the buffer was evaporated by several rounds of lyophilization, and the tryptic peptide mixture was dissolved in 5 μl of 128 mM ammonium carbonate buffer, pH 8.9, and the entire sample was spotted onto a 20 × 20-cm cellulose thin layer chromatography (TLC) plate. The first dimension, thin layer electrophoresis (TLE), was performed at 1.0 kV for 24 min in the same buffer. The plate was then air-dried overnight, after which ascending chromatography was performed in *n*-butyl alcohol:pyridine:acetic acid:water at 15:10:3:12, v/v/v/v. The plate was air-dried, and phosphopeptides were detected by phosphoimaging.

Edman Sequencing—Phosphopeptides localized on TLC plates were recovered from the plate by elution with a solution of formic acid, acetic acid, water, 25:78:897 v/v/v, pH 1.9. The ^{32}P content of each sample was determined by Cerenkov counting. One-tenth of each sample volume was analyzed by phosphoamino acid analysis, and rest of each sample was subjected to Edman degradation as described by Blume-Jensen *et al.* (27). Peptides were coupled to Sequelon-AA membranes, and Edman degradation was performed on an ABI sequencer model 477A. Released phenylthiohydantoin amino acid derivatives from each cycle were spotted on TLC plates, and the radioactivity was quantified by digital imaging after the subtraction of background.

RESULTS

Identification of Phosphopeptides in Tryptic Peptides from Nsp3—Since only a small amount of Nsp3 is synthesized in cells during SFV infection, we used vaccinia-aided transfection to produce sufficient quantities of Nsp3 for phosphorylation analysis. HeLa cells were first infected with the modified vaccinia virus Ankara, which has been engineered to express T7 RNA polymerase (25). Infected cells were then transfected with a plasmid encoding SFV Nsp3 under the control of the T7 promoter. Nsp3 was isolated from cell lysates by immunoprecipitation, liberated from the immunoprecipitation affinity matrix by boiling in Laemmli sample buffer, and further purified by SDS-PAGE. The Nsp3 band visualized on the gel was subjected to in-gel digestion with trypsin. Tryptic peptides were extracted from the gel and desalted using microscale reversed-phase chromatography. Peptide mixtures were eluted directly into a nanospray needle and subjected to mass analysis using a triple quadrupole instrument, which provides high sensitivity for precursor ion scanning. The Q 1 scan displayed in Fig. 1*A* was acquired in the negative ion mode, and it shows a distribution of several signals, indicating good recovery of peptides. A precursor ion scan of m/z (mass/charge) 79 in the negative ion mode is displayed in Fig. 1*B*, and it shows two major peaks at m/z 852 and 916, which were tentatively identified as $[M - 2H]^{2-}$ of peptides Val^{308}–Arg^{322} and Val^{308}–Lys^{323}, respectively (for sequence, see Fig. 1*D*). Each peak appear to carry a single phosphate moiety. Signals at m/z 568 and 610 were identified as $[M - 3H]^{3-}$ counterparts for the 852 and 916 species. In Fig. 1*B*, a series of short peaks (bump-like signals) can be seen between m/z 600 and 1200, and are tentatively identified as a charge series m/z $[M - 14H]^{14-}$ to $[M - 8H]^{8-}$ of peptide Gly^{338}–Lys^{415}. This peptide appears to carry 7–12 phosphates distributed over its 13 potential phosphorylation sites. This assignment was confirmed by double-digestion data as well as site-specific mutation data, as shown below. In Fig. 1*B* (*inset*), a close-up of the $[M - 11H]^{11-}$ species is shown. Fig. 1*C* shows the results from an product ion scan, using a quadrupole-time of flight instrument, done on 853.44 $[M + 2H]^{2+}$ ion (Fig. 1*B*). Using CID analysis, the peptide produced a clear Y-ion series, which allowed for both the identification of the peptide as Val^{308}–Arg^{322} with one phosphate moiety, and the assignment of phosphorylation at Ser^{320}. An expansion of region 450–650 (Fig. 1*C*) shows ions Y3 (m/z 439.22), Y4 (m/z 538.31), and Y5 (m/z 637.33), which are diagnostic of phosphorylation at Ser^{320}, and would be absent if the phosphorylation occurred either at residues Ser^{317} or Thr^{314}. Furthermore, the peptide at 917,49 $[M + 2H]^{2+}$ was analyzed by CID MS, and found to be peptide Val^{308}–Lys^{323}, and it also showed Ser^{320} to be phosphorylated (data not shown). At this point it was evident that the other phosphopeptides observed in the precursor ion scan could not be further analyzed by mass spectrometry alone (see "Discussion").

Double Digestion of Nsp3 by CNBr and Trypsin—As suggested by the precursor ion scan experiment carried out on the tryptic digest of Nsp3, peptide Gly^{338}–Lys^{415} carries 7–12 phosphates, and has a calculated molecular weight between 8838 and 9238 Da. Such large peptide was not amenable to site-specific phosphorylation analysis by mass spectrometry, so in order to reduce the size of this peptide (which contains two methionines), 5 μg (100 pmol) of ^{32}P-labeled Nsp3 was digested in-gel with CNBr, and the resulting peptides were separated by reversed phase chromatography (Fig. 2*A*). Fractions were collected at 1-min intervals, and 0.3 μl of each fraction was spotted to PVDF membrane for autoradiography (Fig. 2*A*). The

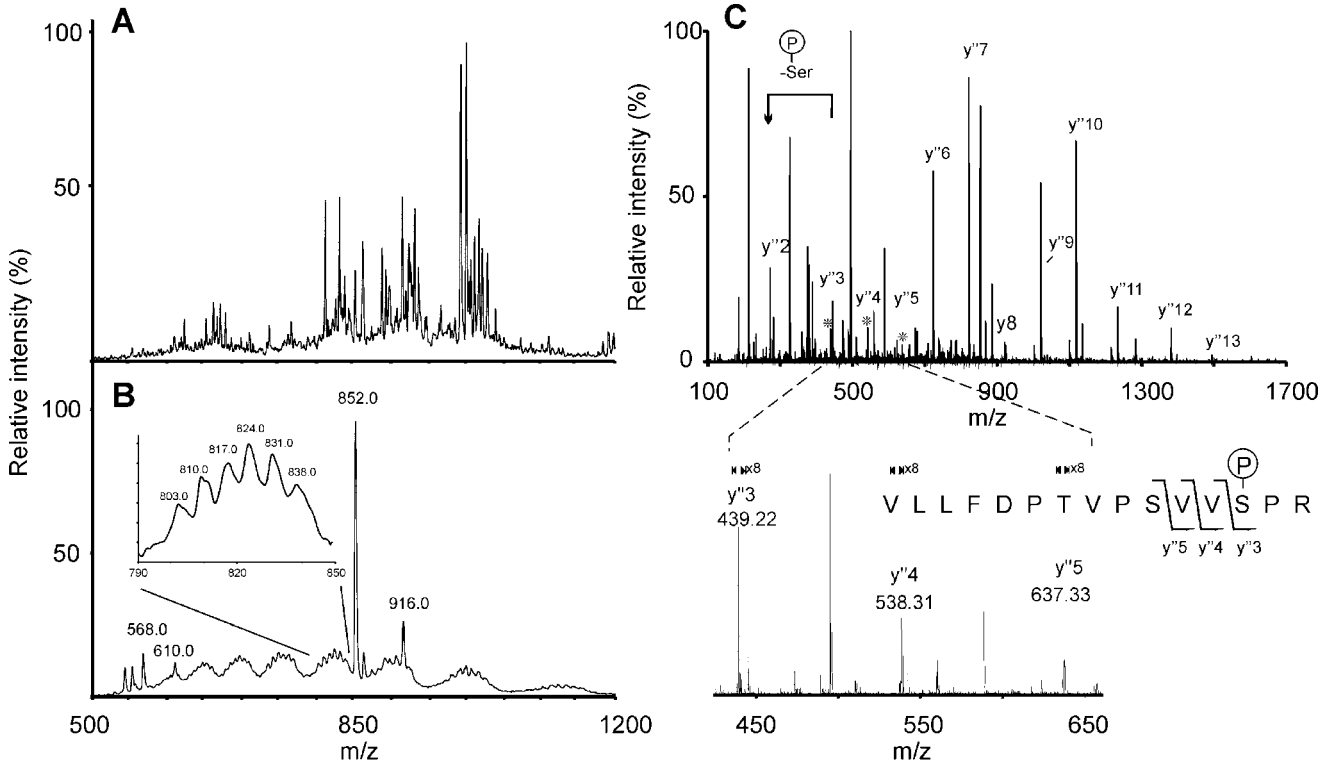

D

```
301 QKVKCEKVLL FDPTVPSVVS PRKYAASTTD HSDRSLRGFD LDWTTDSSST
351 ASDTMSLPSL QSCDIDSIYE PMAPIVVTAD VHPEPAGIAD LAADVHPEPA
401 DHVDLENPIP PPRPKRAAYL ASRAAERPVP APRKPTPAPR TAFRNKLPLT
451 FGDFDEHEVD ALASGITFGD FDDVLRLGRA GA
```

FIG. 1. **Phosphopeptide analysis of Nsp 3 after in-gel trypsin digestion and the amino acid sequence of C-terminal part of Nsp3.** *A*, negative ion ESI Q1 scan of the peptide mixture after elution from the POROS R2 microcolumn. *B*, precursor ion scan of m/z −79 of the same sample showing putative phosphopeptides; *inset*, close-up of m/z 790–850 showing a $[M - 11H]^{11-}$ of a species carrying 7–12 phosphates. *C*, ESI-CID MS analysis of the 853.4 $[M + 2H]^{2+}$ ion. The sequence of the peptide and the phosphorylation site could be determined from a Y-ion series. Diagnostic ions Y3 to Y5, which allow for localization of phosphorylation to Ser^{320}, are marked with an *asterisk* and shown in the *inset*. *Spectra A* and *B* were acquired using a triple-quadrupole instrument, and *spectrum C* using a quadrupole-time of flight instrument. *D*, amino acid sequence of the C-terminal part of SFV Nsp3. Cleavage sites by trypsin (*Trp*) and CNBr are marked with *lines*.

resulting peptides were pooled into three pools according to the elution of radioactivity, and each pool was digested with trypsin. After trypsin digestion, an aliquot of each pool, corresponding to 50 pmol of Nsp3, was separated by microscale RP chromatography, and again fractions were collected, with part of each fraction being subjected to autoradiography. Radioactive fractions were then analyzed by MALDI-TOF mass spectrometry in both positive and negative ion modes in order to identify phosphopeptide candidates. From RP chromatography done on pool 1 (Fig. 2*B*), a series of peptides (1938.0, 2018.0, 2098.0, 2178.0, and 2258.0; $[M - H]^-$, average mass), could be discerned, each separated by 80 Da. According to mass alone, the peptides could not be assigned directly to Nsp3 sequence, even taking into consideration phosphorylation, and possible modifications introduced by CNBr digestion (*e.g.* acid cleavage, oxidation of tryptophans, conversion of methione to homoserine (Hser) without chain cleavage). Signal 1938.8 $[M + H]^+$ (monoisotopic mass), which is the smallest species in this series, was chosen for CID MS analysis, because it would most likely produce the least complex CID MS spectrum compared with other more phosphorylated peptides. A product ion scan of 969.9 $[M + 2H]^{2+}$ was acquired using a quadrupole-time-of-flight instrument, and upon CID the peptide produced a mixed y- and b-ion series, which together identified the peptide as Ser^{356}–Met^{372}. The methione at position 372 was found to be in the open homoserine form (not as in lactone form). This molecular species did not contain phosphates, and it was found to carry an acrylamide adduct on residue Cys^{363} (Cys-propionamide), which is a frequent modification introduced to proteins during SDS-PAGE.

Enrichment of Phosphopeptides by Fe^{3+}-immobilized Metal Chelate Affinity Chromatography Followed by MALDI Mass

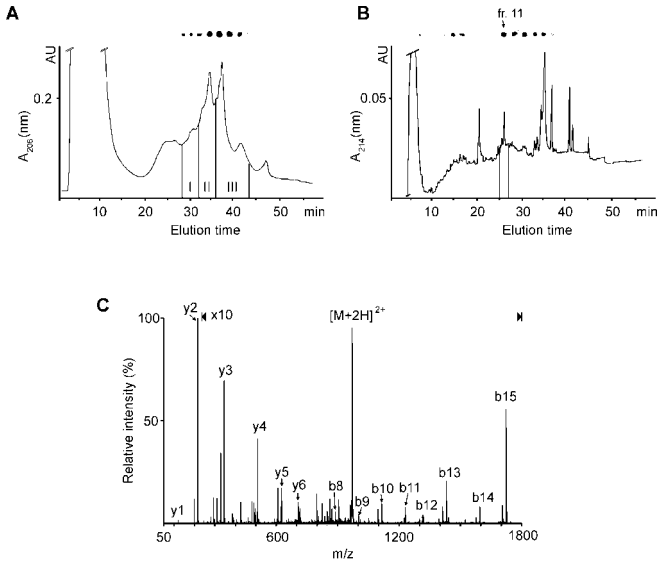

FIG. 2. **Double digestion of Nsp3 with CNBr and trypsin.** *A*, reversed-phase chromatography of an in-gel CNBr-digested, ^{32}P-labeled Nsp3, and radioactivity distribution (*spots* above the chromatogram) in the eluate. Regions 1, 2, and 3, which were pooled separately, are marked on the chromatogram. *B*, microbore RP-HPLC separation of a tryptic digest of pool 1, and radioactivity distribution in the eluate. *C*, ESI-CID MS analysis of the 969.9 $[M + 2H]^{2+}$ ion from fraction 11. The sequence of the peptide could be determined from mixed y- and b-ion series.

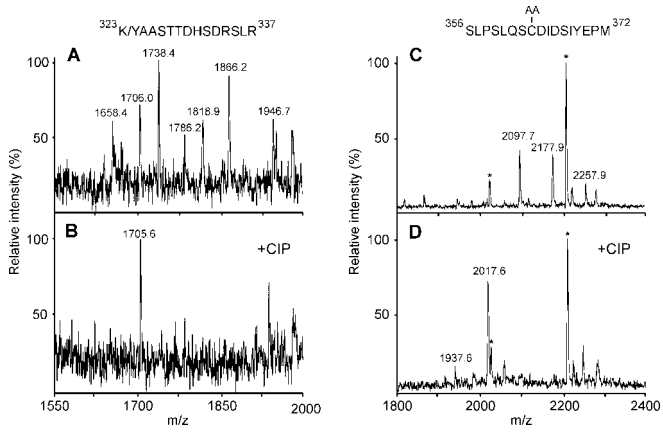

FIG. 3. **MALDI TOF mass spectra of double digested Nsp3 after elution from Fe^{3+}-affinity column combined with on-target dephosphorylation.** *Spectra A* and *B* were acquired in the linear negative ion mode with THAP as the matrix. The sample was then dephosphorylated on the MALDI target, and analyzed again in the linear negative ion mode (*panels B* and *D*). Only the regions containing putative phosphopeptides are shown. In *panel A*, signals *m*/*z* 1658.4, 1738.4, and 1818.9, which were tentatively identified as peptide Tyr^{324}–Arg^{337}, carrying 1, 2, and 3 phosphates, respectively, and signals *m*/*z* 1786.2, 1866.2, and 1946.7, which were tentatively identified as peptide Lys^{323}–Arg^{337}, carrying 1, 2, and 3 phosphates, respectively, could be observed. On-target dephosphorylation of the sample resulted in disappearance of these signals (*B*). In *panel C*, signals 2097.7, 2177.9, and 2257.9 were suggestive of a multiphosphate peptide, which, however, could not be assigned to Nsp3 sequence. After phosphatase treatment (*D*), these signals disappeared and two new signals, 1937.6 and 2017.6, appeared. This signal was found in the liquid chromatography fractions, and identified as Ser^{356}–Met^{372} by CID MS (as shown in Fig. 2).

Analysis and On-target Alkaline Phosphatase Treatment—To facilitate the identification of phosphopeptides, Fe^{3+}-immobilized metal chelate affinity chromatography was used for enrichment of phosphopeptides before MALDI mass analysis. An aliquot of CNBr-trypsin double-digested peptide mixture was passed through a miniature Fe^{3+}-charged POROS MC column, washed and eluted directly onto a MALDI target plate. The eluate was dried under a stream of warm air, dissolved into 1 μl of THAP matrix solution, and rapidly crystallized under vacuum. The sample was analyzed both in the linear negative-ion mode for maximum sensitivity for phosphopeptides, and reflector positive-ion mode for maximum mass accuracy. The crystallized sample was then dissolved and dephosphorylated on the MALDI target plate. After dephosphorylation, the matrix was re-crystallized and subjected to MALDI-TOF mass analysis. Comparison of the mass spectra recorded in the linear negative ion mode before (Fig. 3, *A* and *C*) and after dephosphorylation (Fig. 3, *B* and *D*) revealed several signals attributable to putative phosphopeptides. Signals (Fig. 3*A*) at *m*/*z* 1658.4, 1738.4, and 1818.9 were tentatively identified as peptide YAASTTDHSDRSLR (Tyr^{324}–Arg^{337}), carrying 1, 2, and 3 phosphates, respectively. Signals at *m*/*z* 1786.2, 1866.2, and 1946.7 were tentatively identified as peptide KYAASTTDHSDRSLR (Lys^{323}–Arg^{337}), carrying 1, 2, and 3 phosphates, respectively. These signals disappeared after CIP treatment (Fig. 3*B*). However, no signal corresponding to fully dephosphorylated forms of these peptides could be observed after CIP treatment. This was possibly due to the basic nature of the peptide after dephosphorylation and/or increased salt content of the sample after dephosphorylation. However, a signal at 1706.0 was observed prior and after to CIP treatment, which may be a non-phosphorylated peptide Tyr^{324}–Arg^{337} retained by the Fe^{3+} column, or an unrelated signal having the same *m*/*z* value. Because of these results, assignment of the signals cannot be conclusively made, but further analyses by the phosphopeptide mapping and Edman sequencing confirmed phosphorylation within Tyr^{324}–Arg^{337} (see below). It should be noted that the phosphorylation sites within this sequence could be only determined by using Edman sequencing. Signals at *m*/*z* 2097.7, 2177.9, and 2257.9 were suggestive of a multiphosphorylated peptide, which, however, could not be assigned directly to any peptide of Nsp3. Based on the observations that a similar series of signals were present in the chromatography fractions presented in Fig. 2, the peptide was identified as Ser^{357}–Met^{372} by CID MS. After phosphatase treatment (*D*), these signals disappeared and two new signals, 1937.6 and 2017.6 $[M - H]^-$, appeared, the former representing the fully dephosphorylated peptide and the latter representing a partially dephosphorylated peptide still carrying one phosphate.

Phosphopeptide Mapping of Nsp3 and Its Derivatives—To obtain overall picture of the phosphorylation sites in Nsp3, and to confirm the findings obtained by other methods, Nsp3 and two engineered mutants were analyzed by phosphopeptide mapping. Nsp3 and its mutant forms were labeled with [^{32}P]orthophosphate, immunoprecipitated, and then resolved by SDS-PAGE. Proteins were electrotransferred to nitrocellulose or PVDF membrane, and membrane pieces that contained Nsp3 were excised and subjected to tryptic digestion. Peptides liberated by the digestion were analyzed for radioactive phosphate by TLE/TLC mapping. This analysis revealed three major tryptic phosphopeptides, which are displayed in Fig. 4*A* as spots labeled *a*, *b*, and *c*. Phosphopeptides *a* and *b* in Fig. 4*A* represent about 15% and 2%, respectively, of the total signal as quantified by phosphoimaging. According to phosphoamino acid analysis, phosphopeptide *c* (Fig. 4*A*) was the only peptide containing phosphothreonine (about 25% of total phosphate for *c*), while the other peptides, *a* and *b* in Fig. 4*A*, and *d* and *e* in Fig. 4*B*, contained only phosphoserines (data not shown). Furthermore, the spot representing phosphopeptide *c* migrated very slowly in the second dimension, which was probably due to its relatively large size (78 aa). Peptide spot *c* was reproducibly diffuse, which was most likely caused by heterogeneous phosphorylation. When Nsp3 was digested on PVDF membrane, phosphopeptide mapping revealed the same peptides spots *a*

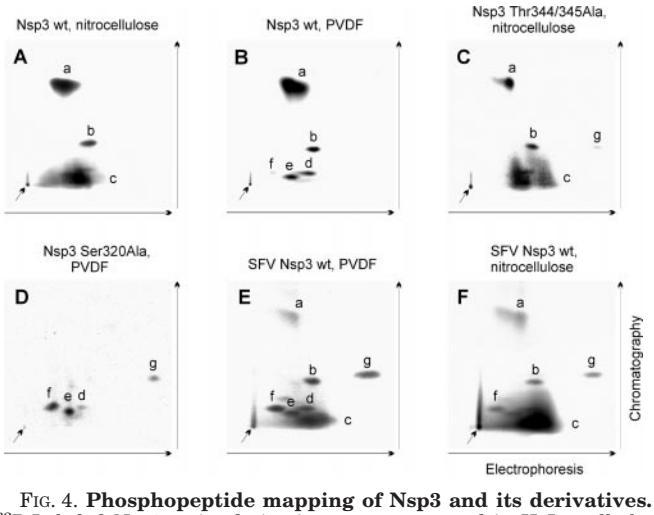

FIG. 4. **Phosphopeptide mapping of Nsp3 and its derivatives.** ^{32}P-Labeled Nsp3 or its derivatives were expressed in HeLa cells by transfection or in BHK cells by infection, analyzed by Western blot, using either nitrocellulose or PVDF membrane. The bands corresponding to Nsp3 produced in HeLa cells on nitrocellulose (*A*) or PVDF membrane (*B*) and Nsp3 mutants Thr^{344} → Ala/Thr^{345} → Ala on nitrocellulose membrane (*C*) and Ser^{320} → Ala on PVDF membrane (*D*), and Nsp3 from SFV-infected BHK cells on nitrocellulose (*E*) or PVDF (*F*) were cut from the membranes and subjected to tryptic digestion. Eluted phosphopeptides were analyzed by two-dimensional phosphopeptide mapping (TLE/TLC) as described under "Experimental Procedures." Samples were applied at the spot marked by *arrows*, and the directions of TLE and TLC runs are marked on the *sides* of the plates.

and *b*, as seen when nitrocellulose membrane was used, but peptide spot *c* appeared not to have been eluted from the PVDF membrane (Fig. 4*B*). In contrast, PVDF membrane appeared to release three other phosphopeptides, spots *d*, *e*, and *f*, which were most likely concealed by peptide *c* in Fig. 4*A*. Nsp3 double mutant, Thr^{344} → Ala/Thr^{345} → Ala showed a peptide-mapping pattern similar to wt Nsp3, except for peptide spot *c*, which appeared somewhat shifted in position (Fig. 4*C*). Since Ser^{320} was identified to be a phosphorylation site using CID MS (Fig. 1*C*), Nsp3 mutant Ser^{320} → Ala was also analyzed by phosphopeptide mapping in an attempt to identify the phosphopeptide(s) that might contain this phosphorylation site. As shown in Fig. 4*D*, this mutation appeared to completely lack the phosphopeptide representing spot *a*, compared with wt Nsp3 analyzed in Fig. 4*B*. This was consistent with the interpretation that phosphopeptide *a* was a tryptic peptide, Val^{308}–Pro^{321}, which included the serine at position 320.

Previously, Peränen *et al*. (18) showed that Nsp3 is phosphorylated at serines and threonines, in a ratio of approximately 2 to 1 in SFV-infected baby hamster kidney cells. In contrast, when HeLa cells are transfected with Nsp3, the ratio between phosphorylated serines and threonines appeared to be higher (approximately 6 to 1; data not shown). To study whether the phosphorylation sites utilized during SFV infection of BHK cells and Nsp3 transfection of HeLa cells were similar, phosphopeptide maps were made using these two conditions. ^{32}P-Labeled Nsp3 derived from SFV infection was treated as described above and analyzed by two-dimensional mapping. As can be seen in Fig. 4 (*E* and *F*), Nsp3 from infected BHK cells showed a similar pattern of phosphopeptides compared with transfected HeLa cells. Although this suggests that both cell types and expression modes utilize similar Nsp3 phosphorylation sites, there are reproducible differences in the relative amount of the phosphopeptides (Fig. 4, *E* and *F*), which may reflect the differences in serine to threonine phosphorylation ratios.

Edman Sequencing—From TLC plates, phosphopeptides *a* through *g* (Fig. 4, *A* and *B*) were extracted for Edman sequencing. In the case of phosphopeptide *c*, only a small sample was taken from the center of the spot and used for further analysis. This precaution was taken to avoid contamination from other phosphopeptides, which may be masked by this diffuse spot. Edman sequencing was performed using an automated sequencer, and released amino acid derivatives were quantified by phosphoimaging. The interpretation of the results for phosphopeptides *a*, *b*, *d*, and *e* was unambiguous. As already concluded from point mutational analysis, and verified by Edman sequencing, phosphopeptide *a* was tryptic peptide Val^{308}–Arg^{322}, and was phosphorylated at Ser^{320} (Fig. 5*A*). Phosphopeptide *b* was tripeptide Ser^{335}–Arg^{337}, which was phosphorylated at Ser^{335} (Fig. 5*B*). Phosphopeptides *d* and *e* appeared to be the same tryptic peptide, Tyr^{324}–Arg^{334}, with or without Lys^{323}, respectively (Fig. 5, *C* and *D*), and both showed that Ser^{327} was phosphorylated. Although the relative amount of ^{32}P in spot *c*, which was analyzed by Cerenkov counting, was similar to amounts in spot *a*, analysis of sample *c* showed a significant reduction in signal generated by Edman sequencing (Fig. 5*C*). Putatively, phosphopeptide *c* was tryptic peptide Gly^{338}–Lys^{415}. This relatively long peptide (78 aa) contained 13 potential phosphorylation sites (8 serines and 5 threonines) and carried from 7 up to 12 phosphates, as evidenced by precursor ion scanning. In addition, this peptide also had a combined total of 15 aspartatic acid and glutamic acid residues, which can covalently attach to Sequelon-AA membranes. Thus, Edman sequencing of this kind of peptide is not likely to produce informative data (see "Discussion"). Phosphopeptides *f* and *g* seen in Fig. 4 (*E* and *F*) could be observed in all the maps; however, their ^{32}P content was too low for further analyses (Fig. 4, *B–D*).

Generation of a Non-phosphorylated Nsp3 Mutant—Based on mass spectrometric, phosphopeptide mapping, and point mutational analysis of Nsp3, phosphorylation sites were demonstrated at serines 320, 327, 332, and 335. From 7 up to 12 potential phosphorylation sites are suggested in peptide Gly^{338}–Lys^{415}, which has a total of 8 serines and 5 threonines. In an effort to better illuminate the phosphorylation sites in peptide Gly^{338}–Lys^{415}, a 26-aa deletion mutant was made that removed residues 343–368. This mutant removed 12 of the 13 potential phosphorylation sites in peptide Gly^{338}–Lys^{415}, while maintaining highly conserved residues such as Tyr^{324}. Remaining phosphorylation sites at serines 320, 327, 332, and 335 were then point mutated to alanines, and the final Nsp3 mutant, Nsp3Δ26+4S→4A, was expressed in HeLa cells. Nsp3Δ26+4S→4A or wt Nsp3 were labeled with [^{35}S]methionine/cysteine, immunoprecipitated, and subjected to SDS-PAGE (Fig. 6, *lanes 1* and *2*, respectively). As can be seen in Fig. 6, the mobility of Nsp3Δ26+4S→4A (*lane 1*) appeared slightly faster than the wt Nsp3 (*lane 2*), and would be indicative of the 26-aa deletion. Although the mutant protein was smaller than the wt Nsp3 protein, the mutations did not appear to have any obvious effects on expression levels as compared with wt Nsp3 protein. This may suggest that the mutant form is as stable *in vivo* as wt Nsp3 protein. Fig. 6 also shows results from labeling Nsp3Δ26+4S→4A and wt Nsp3 transfected HeLa cells with [^{32}P]orthophosphate (Fig. 6, *lanes 3* and *4*, respectively). It appeared that the mutation made in Nsp3Δ26+4S→4A drastically decreased any phosphorylation of the protein (*lane 3*) compared with wt Nsp3 protein (*lane 4*). Assuming that the 26-aa deletion and the four serine to alanine substitutions did not affect the overall conformation of the protein, it appears that most if not all other potential phosphorylation sites, like the one at Thr^{378}, are not phosphorylated to any appreciable amounts. Instead, complete loss of ^{32}P incorporation to the Nsp3Δ26+4S→4A can be observed, which sug-

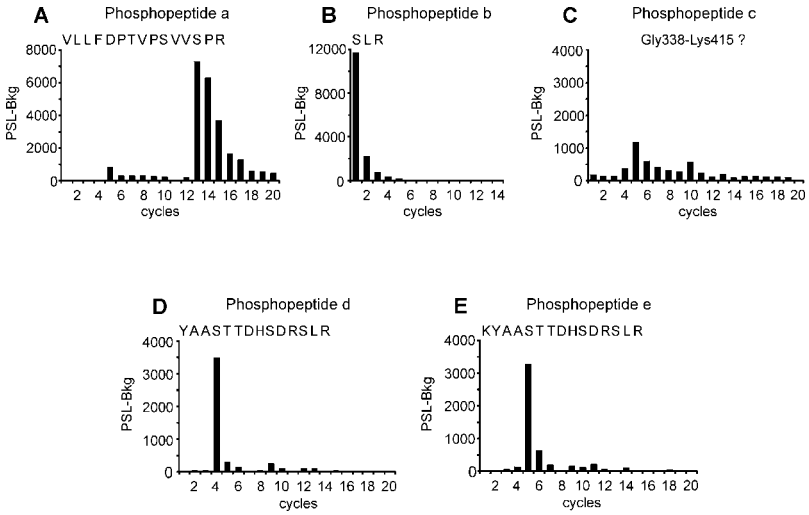

FIG. 5. **Edman sequencing of phosphopeptides from peptide mapping.** Phosphopeptides *a–e* (*panels A–E*) from phosphopeptide mapping (see Fig. 4, *A–D*) were eluted to pH 1.9 buffer, coupled to Sequelon-AA membranes and analyzed by successive cycles of Edman degradation. The amount of ^{32}P label released by each round of sequencing was quantified by phosphoimaging after subtraction of the background.

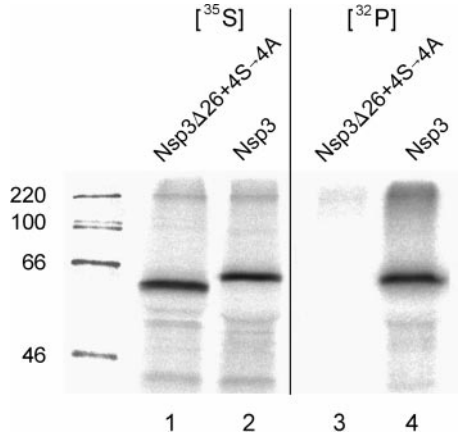

FIG. 6. **Phosphorylation of Nsp3 and internal deletion mutant Nsp3Δ26+4S→4A.** HeLa cells were infected with modified vaccinia Ankara virus and transfected by plasmid encoding Nsp3Δ26+4S→4A (*lanes 1* and *3*) or wild type Nsp3 (*lanes 2* and *4*). The cells were labeled with [^{32}P]orthophosphate or [^{35}S]methionine/cysteine as indicated. Cell extracts were collected, immunoprecipitated with anti-Nsp3 antibody, and analyzed by SDS-PAGE. The proteins were visualized by phosphoimaging. Molecular mass markers (in kDa) are shown on the *left*.

gests that we have succeeded in finding all phosphorylation sites of Nsp3.

DISCUSSION

In this study we have been able to identify most if not all of the phosphorylation sites of SFV Nsp3 by using a combination of analytical techniques. In summary, the main phosphorylation sites appear to be at Ser^{320} and within peptide Gly^{338}–Lys^{415}, which contains 7–12 phosphates distributed over its 13 potential sites. Phosphorylation also appears to occur, albeit to a lesser extent, within peptide Lys^{323}–Arg^{337}, which is phosphorylated at serines 327, 332, and 335. In the case of peptide Val^{308}–Arg^{322}, the assignment of phosphorylation at Ser^{320} was determined by precursor ion scanning, MALDI, tandem mass spectrometry, and Edman sequencing.

In contrast, peptide Gly^{338}–Lys^{415} was more problematic for determining exact sites of phosphorylation. Although it was determined by mass spectrometric method (precursor ion scanning) that peptide Gly^{338}–Lys^{415} carried from 7 up to 12 phosphates, its relatively large size (78 aa) and extensive phosphorylation did not make it amenable to further structural analysis by mass spectrometric methods. Such a peptide creates problems, which fall into two categories: 1) the peptide is too heavily phosphorylated to be ionized in the positive ion mode, which is a prerequisite for performing CID MS analysis; and 2) the peptide is far too large to yield an informative fragmentation pattern. In addition, peptide Gly^{338}–Lys^{415} was impossible to effectively analyze by Edman degradation sequencing. For Edman degradation, the peptide of interest is covalently attached to an arylamine membrane via its carboxyl groups (as well from carboxyl end as Asp and Glu residues). The peptide is attached to the membrane via any carboxyl groups by random, and every time the sequencing proceeds to a carboxyl group containing residue, part of the peptide pool is released, which can be interpreted as release of phosphoamino acid. Additionally, big peptides are more likely to undergo unspecific chain fragmentation under the Edman degradation conditions than small ones. The larger the peptide, and the more acidic amino acids (Asp or Glu) the peptide contains, the more problematic the peptide is for the Edman sequencing approach. The peptide Gly^{338}–Lys^{415} is both large (approximately 8 kDa) and acidic (11 Asp and 4 Glu residues), and the problems arising with sequencing are well demonstrated in the sequence analysis of spot *c* (Fig. 4*A*), where the peptide seems to leak radioactivity in almost every cycle. However, from the mass spectrometric analysis, we know that the peptide carries up to 12 phosphates on its 13 potential phosphorylation sites. Furthermore, after CNBr cleavage and trypsin digestion, the C-terminal part of the phosphorylated region, peptide Ser^{356}–Met^{372} appeared to have 0–4 phosphates. This indirectly indicates that the N-terminal 18-aa peptide Gly^{338}–Met^{355}, carrying 8 potential phosphorylation sites, probably contained at least 7 phosphates in the case where the former peptide is not phosphorylated at all (since the tryptic peptide Gly^{338}–Lys^{415} contains 7–12 phosphates as judged by precursor ion scanning experiments). On the basis of these data, we assume that the Ser and Thr residues in region Thr^{344}–Thr^{354} are the most heavily phosphorylated residues in this peptide, although these data do not give direct evidence regarding the phosphorylation of Thr^{378}. However, assuming that the 26-aa internal deletion of Nsp3Δ26+4S→4A did not affect the accessibility of Thr^{378} to kinase(s) by causing conformational changes, it appears that in this Nsp3 derivative Thr^{378} is not modified by phosphorylation (*i.e.* Nsp3Δ26+4S→4A does not incorporate [^{32}P]orthophosphate even though Thr^{378} is present in the sequence).

The peptides Lys^{323}–Arg^{337} and Tyr^{324}–Arg^{337}, both of which contain the same potential phosphorylation sites (serines at 327, 332, and 335) went unnoticed in the precursor ion scanning experiments, most likely because their signals were too weak to overcome the signals arising from peptide Gly^{338}–Lys^{415} peptide in its multiple charged states. The weak signal

from Lys^{323}–Arg^{337} and Tyr^{324}–Arg^{337} was probably due to signal distribution over three different phosphorylation states, their sodium adducts, and their different charge states. These peptides were only observed with MALDI/CIP experiments, and further site-specific information about phosphorylated residues could only be obtained by Edman sequencing. Data from either the MALDI/CIP experiment or Edman sequencing alone would not have been sufficient for unequivocal identification of the phosphorylated residues in this region of Nsp3.

The tripeptide Ser^{335}–Arg^{337} could not be observed by MALDI/CIP experiment, probably due to matrix signals in the mass region of the peptide. In addition, this peptide could not be identified in the precursor ion scanning experiments, which is most likely due to the hydrophilic nature of the peptide. Although peptide Ser^{335}–Arg^{337} was probably lost in the desalting step prior to the mass analysis, it was successfully analyzed by Edman sequencing (Fig. 5*B*).

Even though several mass spectrometric methods for phosphorylation site analysis of subpicomole amounts of protein have been presented (20–23, 28), the methods were not fully applicable for all of the phosphopeptides found in this study for the reasons discussed above. The levels of sensitivity achieved in all the techniques used here were at the subpicomole level, as determined by standard proteins (such as casein) used during validation steps. For mass spectrometric analysis, roughly 10 pmol of protein was used for each experiment, which was plenty for most of the analysis. Since several methodological approaches had to be used to find out all phosphorylation sites in the Nsp3 sequence, we consumed roughly 150–200 pmol of material to complete all of the experiments presented in this study.

In summary, we can conclude that, in the case of Nsp3, several independent methods were needed to localize phosphorylated residues, and any of these methods used alone would have resulted in only partial information. In addition, the use of deletion and point mutations were a valuable tool for confirming results obtained by analytical approaches. Furthermore, each analytical method used to analyze protein phosphorylation has its own pitfalls. For mass spectrometric methods, the phosphopeptides must be large or hydrophobic enough to allow for desalting without significant losses (22). Although digested peptides can be analyzed without desalting step by MALDI mass spectrometry (23), small peptides (below 600 Da) are likely to be covered under the matrix signals. Large peptides or peptides containing multiple phosphates are not likely to produce informative fragmentation patterns, which would allow for site-specific assignment of phosphorylation over the sequence. Edman sequencing data alone are not always unequivocal. Two or more peptides in the protein sequence may produce similar radioactivity distribution profiles after sequencing. Two-dimensional TLE/TLC phosphopeptide mapping gives a good overview of the number of phosphopeptides present in the protein of interest, but does not offer much in the way of exact phosphorylation sites. The two-dimensional peptide mapping is of great use when used in combination with the Edman sequencing approach or/and point mutational analysis. Point mutational approaches carry the risk of false assignments in the cases when the point mutation causes a conformational change in the protein, which in turn prevents the phosphorylation of the protein, even though the mutated site would not actually be a phosphorylated site. As an example, when threonines 344 and 345 or Ser^{320} in the Nsp3 were mutated to alanines, the overall phosphorylation of the protein dropped by approximately 50% ,[2] even though each of these amino acids carry clearly less than 15% of total phosphate in the wt Nsp3. This suggests that the phosphorylation of these sites affects the phosphorylation of other sites, thus giving a false picture of overall phosphorylation of Nsp3. Taken together, one should use combination of several methods to be able to get a reliable picture of phosphorylation of the protein of interest.

From this study, it appears that most of the SFV Nsp3 phosphorylation sites occur in its variable C-terminal region. Even Ser^{320}, one of the main phosphorylation sites of SFV Nsp3, is not conserved in other alphaviruses. SIN Nsp3 is even more heavily phosphorylated on serines and threonines than its relative SFV Nsp3. This extensive phosphorylation of SIN Nsp3 leads to the formation of several species with different electrophoretic mobilities (19). Although SIN Nsp3 phosphorylation has not been investigated as extensively as SFV Nsp3 has been in this report, deletions made in the non-conserved C-terminal region of SIN Nsp3 appeared to significantly reduce its phosphorylation (29). In the SIN Nsp3 non-conserved C-terminal domain, there are two separate Ser/Thr-rich areas, which could be highly phosphorylated, causing the electrophoretically distinguishable forms observed. Furthermore, one of the kinases involved in the phosphorylation of SIN Nsp3 has been suggested to be casein kinase II (19). This could be the same kinase that is involved in the phosphorylation of SFV Nsp3 residues Ser-327, Ser-335, and all of the potential Ser/Thr residues in region Thr^{344}–Ser^{367}, as suggested by aa sequences around these sites. The consensus sequence for casein kinase II is Asp, Glu, or phosphorylated serine at the position one to three amino acids toward the C-terminal side of to the phosphorylation acceptor serine or threonine (30). However, phosphorylation sites at Ser^{320} and Ser^{335} do not appear to be associated with the casein kinase II consensus sequence. Instead, they appear to be potential sites for protein kinase C, as well as Ser^{332}, since they all have the consensus sequence of Ser/Thr-*X*-Arg/Lys (30). Furthermore, both casein kinase II and protein kinase C have been reported to phosphorylate viral nonstructural proteins among negative-strand RNA viruses (2, 31–34).

The primary objective of this study was to determine the major sites of Nsp3 phosphorylation at first the peptide level, and if possible at the amino acid level. To reach our goal, we combined a number of analytical methods to generate determinate results regarding most if not all phosphorylation sites in Nsp3. Deletion and point mutations of the phosphorylated residues resulted in non-phosphorylated derivatives of Nsp3 incapable of incorporating [^{32}P]orthophosphate (Fig. 6). These results will allow us to alter the native phosphorylation patterns of Nsp3 in the context of SFV for the ultimate goal of testing effects of phosphorylation on SFV replication and pathogenesis.

Acknowledgments—We are grateful to Dr. Ulf Hellman and Christer Wernstedt from Ludvig Institute of Cancer Research for performing the Edman sequencing analysis. We also thank Dr. Nisse Kalkkinen for valuable discussions over methodological aspects throughout this study, as well as Dr. Jari Helin, Dr. Tero Ahola, and Dr. Kristiina Mäkinen for their critical review of this manuscript.

REFERENCES

1. Leader, D. P, and Katan, M. (1988) *J. Gen. Virol.* **69,** 1441–1464
2. Barik, S., and Banerjee, A. K. (1992) *Proc. Natl. Acad. Sci. U. S. A.* **89,** 6570–6574
3. Chattopadhyay, D., and Banerjee, A. K. (1987) *Cell* **49,** 407–414
4. Kääriäinen, L., Takkinen, K., Keränen, S., and Söderlund, H. (1987) *J. Cell Sci. Suppl.* **7,** 231–250
5. Strauss, J. H., and Strauss, E. G. (1994) *Microbiol. Rev.* **58,** 491–562
6. Laakkonen, P., Hyvönen, M., Peränen, J., and Kääriäinen, L. (1994) *J. Virol.*

[2] H. Vihinen, T. Ahola, M. Tuittila, A. Merits, and L. Kääriäinen, submitted for publication.

68, 7418–7425
7. Ahola, T., and Kääriäinen, L. (1995) *Proc. Natl. Acad. Sci. U. S. A.* **92,** 507–511
8. Hardy, W. R., and Strauss, J. H. (1989) *J. Virol.* **63,** 4653–4664
9. Gomez de Cedrón, M., Ehsani, N., Mikkola, M., Garcia, J., and Kääriäinen, L. (1999) *FEBS Lett.* **48,** 19–22
10. Vasiljeva, L., Merits, A., Auvinen, P., and Kääriäinen, L. (2000) *J. Biol. Chem.* **275,** 17281–17287
11. Barton, D. J., Sawicki, S. G., and Sawicki, D. L. (1988) *J. Virol.* **62,** 3597–3602
12. Lemm, J. A., Rümenapf, T., Strauss, E. G., Strauss, J. H., and Rice, C. M. (1994) *EMBO J.* **13,** 2925–2934
13. Shirako, Y., and Strauss, J. H. (1994) *J. Virol.* **68,** 1874–1885
14. Wang, Y.-F., Sawicki, S. G., and Sawicki, D. L. (1994) *J. Virol.* **68,** 6466–6475
15. LaStarza, M. W., Lemm, J. A., and Rice, C. M. (1994) *J. Virol.* **68,** 5781–5791
16. Koonin, E. V., and Dolja, V. V. (1993) *Crit. Rev. Biochem. Mol. Biol.* **28,** 375–430
17. Pehrson, J., and Fuji, R. (1998) *Nucleic Acids Res.* **26,** 2837–2842
18. Peränen, J., Takkinen, K., Kalkkinen, N., and Kääriäinen, L. (1988) *J. Gen. Virol.* **69,** 2165–2178
19. Li, G., La Starza, M. W., Hardy, W. R., Strauss, J. H., and Rice, C. M. (1990) *Virology* **179,** 416–427
20. Annan, R. S., and Carr, S. A. (1997) *J. Protein Chem.* **16,** 391–402
21. Wilm, M., Neubauer, G., and Mann, M. (1996) *Anal. Chem.* **68,** 527–533
22. Neubauer, G., and Mann, M. (1999) *Anal. Chem.* **71,** 235–242
23. Zhang, X., Herring, C. J., Romano, P. R., Szczepanowska, J., Brzeska, H., Hinnebusch, A. G., and Qin, J. (1998) *Anal. Chem.* **70,** 2050–2059
24. Peränen, J. (1991) *J. Gen. Virol.* **72,** 195–199
25. Wyatt, L. S., Moss, B., and Rozenblatt, S. (1995) *Virology* **210,** 202–205
26. Nyman, T. A., Kalkkinen, N., Tolo, H., and Helin, J. (1998) *Eur. J. Biochem.* **15,** 485–493
27. Blume-Jensen, P., Wernstedt, C., Heldin, C.-H., and Rönnstrand, L. (1995) *J. Biol. Chem.* **270,** 14192–14200
28. Carr, S. A., Huddleston, M. J., and Annan, R. S. (1996) *Anal. Biochem.* **239,** 180–192
29. LaStarza, M. W., Grakoui, A., and Rice, C. M. (1994) *Virology* **202,** 224–232
30. Kennelly, P., J., and Krebs, E. G. (1991) *J. Biol. Chem.* **266,** 15555–15558
31. Huntley, C. C., De, B. P., and Banerjee, A. K. (1997) *J. Biol. Chem.* **272,** 16578–16584
32. Gupta, A. K., Blondel, D., Choudhary, S., and Banerjee, A. K. (2000) *J. Virol.* **74,** 91–98
33. Das, T., Schuster, A., Schneider-Schaulies, S., and Banerjee, A. K. (1995) *Virology* **211,** 218–226
34. Liu, Z., Huntley, C. C., De, B. P., Das, T., Banerjee, A. K., and Oglesbee, M. J. (1997) *Virology* **232,** 198–206